Structure of ^{23}F via β decay of ^{23}O

C. S. Sumithrarachchi,[1,2,*] D. J. Morrissey,[1,2] B. A. Brown,[1,3] A. D. Davies,[1,3] D. A. Davies,[1,2] M. Fancina,[1] E. Kwan,[1,3] P. F. Mantica,[1,2] M. Portillo,[1] Y. Shimbara,[1] J. Stoker,[1,2] and R. R. Weerasiri[1,2]

[1]*National Superconducting Cyclotron Laboratory, Michigan State University, East Lansing, Michigan 48824, USA*

[2]*Department of Chemistry, Michigan State University, East Lansing, Michigan 48824, USA*

[3]*Department of Physics and Astronomy, Michigan State University, East Lansing, Michigan 48824, USA*

(Received 28 September 2006; published 15 February 2007)

The nuclear states in ^{23}F have been investigated following the β decay of ^{23}O. The measurement of ^{23}O was carried out at the National Superconducting Cyclotron Laboratory using fragments from the reaction of a ^{48}Ca beam in a Be target. The half-life and total neutron emission probability were determined to be 97(8) ms and 7(2)%, respectively, for ^{23}O β decay. Ten γ-ray decays in ^{23}F and a single γ-ray in ^{22}F were observed to establish the β decay scheme for ^{23}O. Shell model calculations are in reasonable agreement with the measured β branching and B(GT) values for the lowest energy state. The excitation energies of the first $1/2^+$ and $3/2^+$ states have been determined to be 2243(8) and 4066(16) keV, respectively, indicating a widening of the $5/2^+$–$1/2^+$ state gap in ^{23}F. The decay scheme of the largest contaminant ^{26}Ne in the experiment was established.

DOI: 10.1103/PhysRevC.75.024305 PACS number(s): 23.40.−s, 21.60.Cs, 23.20.Lv, 27.30.+t

I. INTRODUCTION

The disappearance of traditional magic numbers and the appearance of new magic numbers in approaching the drip line are not clearly understood. The study of neutron-rich fluorine isotopes can provide important information on the variation of nuclear shell structure between the doubly magic oxygen isotopes and the island of inversion region in the nuclear landscape. The knowledge of nuclear structure, in particular in ^{23}F, is important as it should be sensitive to the s and d orbital splitting. ^{23}F also has the structure of a single proton outside the reported doubly magic ^{22}O [1,2]. The present work focused on the β-delayed neutrons and γ rays from ^{23}O β decay to establish the energies of neutron bound and unbound states in ^{23}F. This paper presents the study on β decay of ^{23}O using a neutron spectroscopic array. The results were used to establish the β decay scheme for ^{23}O that are compared with shell model calculations.

Mueller *et al*. reported a total neutron emission probability (P_n) of 31(7)% for the β decay of ^{23}O with a half-life of 82(37) ms, which is the only measurement for the half-life to date [3]. An upper limit for P_n of 29% was subsequently published by Reeder *et al*. [4]. There is no spectroscopic information for the β decay of ^{23}O at present, although there are several theoretical estimates of the half-life of ^{23}O that range from 12.8 to 196 ms [3]. All of the predicted P_n values for ^{23}O β decay were close to 30% and thus agreed with the experimental values with the exception of a value predicted by Wildenthal *et al*., which was only 2% [5]. The energy levels in the daughter of ^{23}O β decay were measured using the heavy-ion transfer reaction ^{22}Ne(^{18}O, ^{17}F)^{23}F by Orr *et al*. [6]. Six energy levels were observed in ^{23}F, in which the ground state and the second and third excited states were assigned to be spin and parity of $5/2^+$, $7/2^+$, and $9/2^+$, respectively, based on shell model calculations. The ground state in ^{23}F was confirmed to be $5/2^+$ by Sauvan *et al*. [7]. Two excited states at 3810 and 2900 keV deexcited by a cascade of γ rays at 910 and 2900 keV in ^{23}F have been reported by Belleguic *et al*. [1] using ^{36}S fragmentation reactions with in-beam γ spectroscopy. These two states were assigned as $7/2^+$ and $9/2^+$, respectively, by comparison with the shell model. Michimasa *et al*. recently reported studies of the excited states in ^{23}F using three kinds of reactions, namely, ^{4}He(^{22}O, $^{23}F\gamma$), ^{4}He(^{23}F, $^{23}F\gamma$) and ^{4}He(^{24}F, $^{23}F\gamma$) [8]. The γ-ray decay scheme was established up to 7 MeV based on $\gamma - \gamma$ coincidence measurements. The energy levels at 2268(12) and 4059(11) keV were tentatively assigned to be $1/2^+$ and $3/2^+$, respectively. The spins and parities for other states are unknown, and no negative parity states in ^{23}F have been observed at present. The ground state of ^{23}O is known to be $1/2^+$ [7], so we expect β decay feeding predominately to excited states because direct feeding to the ground state would be a first forbidden decay.

II. EXPERIMENTAL

The experiment was carried out at the National Superconducting Cyclotron Laboratory of Michigan State University. The radioactive beam of ^{23}O was produced by projectile fragmentation of a 140 MeV/nucleon ^{48}Ca beam in a 846 mg/cm^2 thick Be target placed at the object position of the A1900 fragment separator. The fragments were separated by the A1900 separator using a combination of two magnetic bends (magnetic rigidities: 4.497 and 4.210 Tm) along with a 825 mg/cm^2 Al wedge placed at the middle image position of the A1900, and a relatively narrow momentum acceptance ($\Delta p/p = 0.5\%$). A detailed description of the device and method is given in Ref. [9]. The secondary beam was a cocktail beam consisting of ^{23}O, ^{26}Ne, ^{24}F, and ^{21}N with fractions given in Table I. In addition, ^{16}C and ^{17}N radioactive beams used to calibrate the neutron spectroscopic array were produced separately by changing the magnetic rigidities of the A1900 using the same target and wedge.

*Electronic address: chandana@nscl.msu.edu

TABLE I. Beam purity of ^{23}O experiment from the A1900 and in the implantation detector.

Nuclide	A1900 Purity[a](%)[b]	Implantation detector Purity[c](%)	Literature Half-life[d] (ms)
^{23}O	16.8	14.2	82(37)
^{26}Ne	62.2	83.1	192(6)
^{24}F	7.4	2.1	400(50)
^{21}N	1.5	0.6	85(7)

[a]At the A1900 focal plane from the TOF and energy loss measurement.
[b]^{25}F, ^{27}Ne, ^{10,11,12,13}Be, ^{7,8,9}Li, and ^{6}He contribute to the remaining 12.1%.
[c]Taken from the difference in counts of silicon detectors.
[d]Taken from Ref. [10].

The decay data were measured in a beam-on/beam-off batch mode. The beam was pulsed on for a period of 300 ms to collect nuclides in the implantation detector, and β decay was monitored during a beam-off period of 300 ms. The beam-on/beam-off period was selected based on the half-life value of ^{23}O in the literature [3]. The experimental station consisted of an implantation detector, an array of 16 neutron time-of-flight (TOF) detectors and eight γ-ray detectors. The fragments passed into air through a kapton window, followed by a silicon detector and an aluminum degrader before reaching the implantation detector. The implantation detector (3 mm plastic scintillator) produced a start signal for the neutron and γ-ray detectors at the detection of a β decay event during the beam-off period. On-line particle identification was performed based on the time of flight from the production target and energy loss information from the silicon detectors. A second silicon detector was placed approximately 8 cm after the implantation detector to monitor particles that punched through. An aluminum degrader was placed before the implantation detector and adjusted to a thickness of 11.412 mm so that ^{23}O was fully stopped in the implantation detector. The information from both silicon detectors was used to determine the composition of the implanted beam given in Table I.

Sixteen neutron detectors were used to measure β-delayed neutrons from ^{23}O β decay. The detectors were curved with a radius of 1 m to get an equal flight path for neutrons from the implantation detector, which was located at the center of the array. The details of the design of the neutron bar array and the calibration procedures for energy and efficiency can be found in Refs. [11,12]. The neutron detection efficiency function was defined by well-known β-delayed neutrons from ^{16}C and ^{17}N, and three Monte Carlo calculated data points. The total neutron efficiency was found to be 2.26% at 1.0 MeV.

β-delayed γ-rays were detected using eight detectors from the segmented germanium array (SeGA) [13]. The detectors were placed in a ring structure where the detector crystals were parallel to the beam at a radius of 14 and 19.2 cm away from the implantation detector. The SeGA detectors were calibrated using off-line sources of ^{60}Co, ^{207}Bi, and ^{152}Eu, and the well-known γ-rays from the daughters of the impurities. The total γ-ray efficiency of the SeGA detectors was measured to be 1.9% at 1 MeV.

III. RESULTS

A. Total number of β decay events

The total number of β decay events detected by the implantation detector was determined by fitting the β decay curve with a function that contains contributions from the decays of all implanted nuclides and their decay chains. The model was written for each implanted decay series using Bateman equations [15] and included the growth of each nuclide during the beam-on period. The nuclides that did not decay during the beam-off period were added to the next cycle. Implantation purity ratios, taken from the measurement of silicon detectors, were used to fix the relative initial activities of the implanted isotopes. The half-lives of all daughters and granddaughters, and the half-life of ^{21}N, which are reported in the literature [10], were kept as constants through the fitting procedure. The half-lives of ^{26}Ne and ^{24}F, which were deduced from the γ-ray gated decay curves (see below), were also added to the model as fixed values. In addition, the neutron emission probabilities of ^{24}F and ^{21}N were included by using the values of 5.9% and 81%, respectively, as reported in the literature [10]. Four parameters were left as variables: the half-life of ^{23}O, the implantation rate of ^{26}Ne, the neutron emission probability of ^{23}O, and a constant background. The individual contributions to the decay from each implanted nuclide are shown in Fig. 1 with the total daughter and granddaughter contributions plus the background. The number of β decay events extracted by integrating the individual components are given in Table II along with the half-lives and their uncertainties from different sources. The half-life values and the P_n value of ^{23}O were found to be 102(23) ms and 11(9)% by the fitting, respectively. The large number of activities present in the detector does not allow precise measurement of the half-lives in the bulk activity.

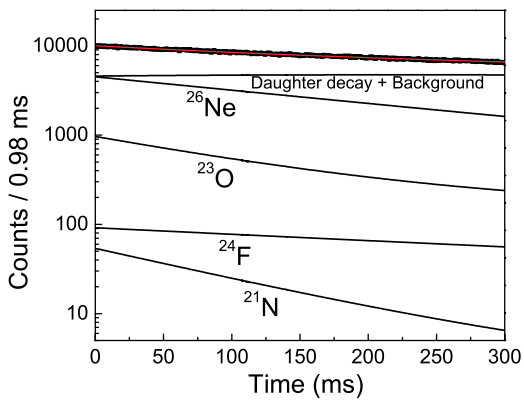

FIG. 1. (Color online) β decay curve of ^{23}O. The total decay curve, individual decay components of the implanted ^{26}Ne, ^{23}O, ^{24}F, and ^{21}N, and background plus all decay contributions of daughter and granddaughter decay are shown.

TABLE II. Detected β decay events from ^{23}O experiment.

Nuclide	Total number of events	Half-life (ms)
^{23}O	$1.47(4) \times 10^5$	102(23)[a]
^{26}Ne	$8.61(2) \times 10^5$	192(4)[b]
^{24}F	$2.21(7) \times 10^4$	384(16)[b]
^{21}N	$6.53(5) \times 10^3$	85(14)[c]

[a]By fitting the decay curve, see the text.
[b]γ-ray gated half-lives from present work.
[c]Taken from Ref. [14].

B. Neutron and γ-ray measurement

The total neutron TOF spectrum measured during the beam-off period and corrected for the constant-fraction discriminator (CFD) walk in all of the detectors in the neutron spectroscopic array is shown in Fig. 2. The position of the β-γ prompt peak provides the time zero reference point for the TOF spectrum. Cosmic rays predominately propagate in the opposite direction through the detection system and trigger the electronics at shorter times relative to the βs to produce the cosmic-ray peak in Fig. 2. No neutron peaks can be observed within the detection limits. The lower and upper detection limits are approximately 360 and 8000 keV, respectively. Since the energy window available for β decay into the neutron unbound states is limited to 3750 keV (channel number 112), the energies of neutrons are within the upper detection limit. It is possible that low energy β-delayed neutrons from β decay of ^{23}O were below the lower energy detection limit of the neutron bar array and a search for the γ-rays that originated from the β-delayed neutron daughter decay was undertaken.

Figure 3 shows the γ-ray spectrum obtained in coincidence with the β decay of the ^{23}O cocktail during the beam-off period. The peaks are labeled with their parent nucleus and energy in keV. The β decay of ^{23}O leads the mass $A = 23$ decay chain yielding the decays of ^{23}F and ^{23}Ne. The γ-ray transitions at 493, 816, 1017, 1701, 1822, 1920, 2132, 2316, 2415, 2734, 3432, and 3831 keV were identified from the β decay of ^{23}F

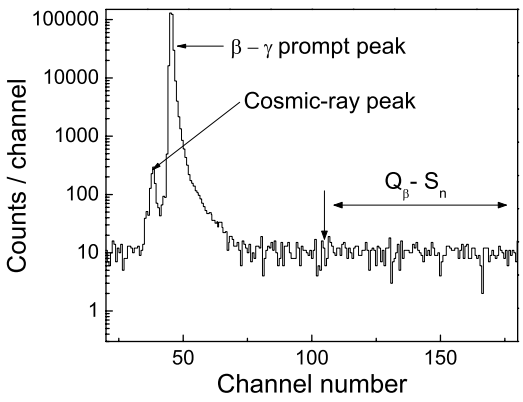

FIG. 2. β-delayed neutron TOF spectrum of ^{23}O obtained by adding all neutron detectors in the array, showing peaks due to cosmic-ray interaction with neutron detectors and the β-γ prompt, and indicating upper limit of the β decay energy window to the neutron unbound states.

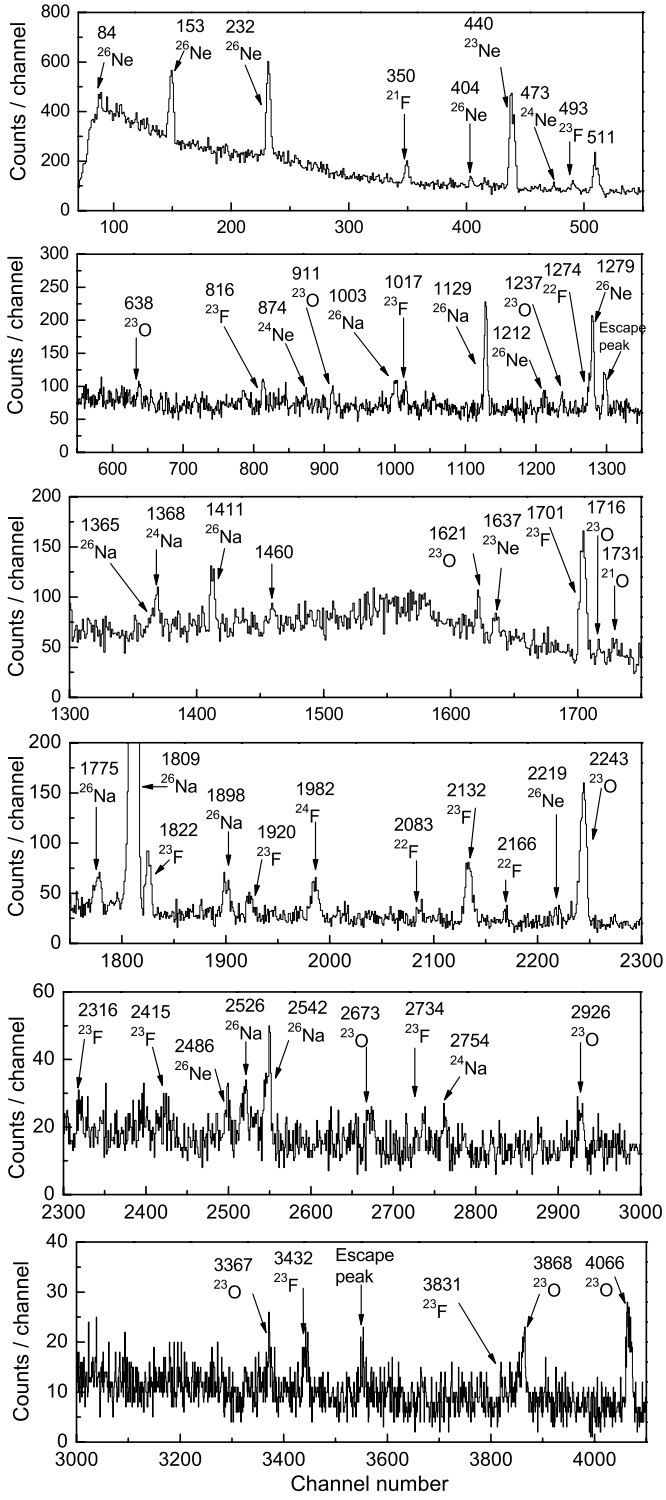

FIG. 3. β-γ coincidence spectrum of the implanted nuclei. γ-ray peak energies are given in keV with their β decay assignments.

based on the previous ^{23}F β decay measurements [14]. The assignments were reconfirmed by determining the gated half-lives for peaks that were statistically significant. Two γ-rays from ^{23}Ne β decay, the granddaughter of ^{23}O, were observed at 440 and 1637 keV with the emission probabilities of 33.0% and 1.1%, respectively. These observations were also in good

agreement with the literature values [14]. The γ-ray transitions from the decay of the impurities in the cocktail beam, such as ^{26}Ne, ^{24}F, and ^{21}N, and their daughters and granddaughters are shown and labeled in Fig. 3. The γ-ray transitions associated with the $A = 26$ decay chain will be addressed separately below. In addition, a γ-ray at 1980 keV was identified from the β decay of ^{24}F, which was also reported in Ref. [14]. The gated half-life of 384(16) ms confirms the assignment. A few γ-rays from the $A = 21$ decay chain determined in previous experiments are also labeled in Fig. 3.

Although β-delayed neutrons from ^{23}O β decay were not observed, γ-ray peaks associated with the β decay of ^{22}F, the β-delayed neutron daughter of ^{23}O, were observed at 1274, 2083, and 2166 keV. These weak transitions had an intensity ratio of 5:4:3. This observation leads to the conclusion that at least one of the ^{22}F states is populated by β-delayed neutron decay of ^{23}O since nuclides with $A = 22$ were not implanted. Excited states in ^{22}F were studied previously in β decay of ^{22}O [16], and ^{22}Ne(^{3}He, t) and ^{22}Ne(^{7}Li, ^{7}Be) reactions [17]. A weak γ-ray at 638 keV was observed that is consistent with neutron feeding of the 3^+ state. The γ-ray at 72 keV in cascade with the 638 keV transition was not seen because of the threshold of the SeGA detectors. Thus, although the neutrons were not observed as discussed above, the observation of the $A = 22$ decay chain and a weak transition in ^{22}F indicate a total β-delayed neutron emission probability at the level of 7(2)%, which was calculated by considering the total β decay of ^{22}F derived from the observed γ-ray activities in ^{22}Ne. Note that the parent and daughter activities in this decay series were saturated during the 30-min-long runs.

The relatively strong γ-ray transitions of 1621, 2243, 2673, 2926, 3868, and 4026 keV were identified from the β decay of ^{23}O, which agree with previous work [1,8]. The gated half-lives were obtained by fitting a single exponential plus background to the gated decay curves, shown in Fig. 4. The deduced gated half-lives are shown in the figure and are labeled by γ-ray energy. The weighted average of the gated half-lives was 97(8) ms. Although the half-life of ^{21}Na is 85(7) ms, the above γ-ray transitions cannot be attributed to the ^{21}Na β decay since the number of implanted nuclides was not high enough to produce such strong peaks. Four γ-rays at 912, 1237, 1716, and 3367 keV were also attributed to ^{23}O β decay based on the work of Belleguic *et al.* [1] and Michimasa *et al.* [8]. The γ-ray at 912 keV was in good agreement with both previous measurements. The transitions at 1237, 1716, and 3367 keV also matched within uncertainties with the reported transitions in Ref. [8]. γ-ray peaks at 2003, 3445, 3985, and 4732 keV reported in the nuclear reaction study were not observed in the present work.

C. ^{26}Ne analysis

The largest implanted contaminant, ^{26}Ne, decays to ^{26}Na, which subsequently decays to the stable nucleus ^{26}Mg. This nucleus was recently studied by Weissman *et al.* [18] and we will only briefly report our confirmation of this work with new shell model calculations. Eight γ rays associated with the daughter of ^{26}Ne β decay known from the literature [14] were observed, and they were labeled in Fig. 3 by their energy and the parent nuclide. With the exception of the 2219 keV γ-ray, the other transitions in Table III were attributed to the β decay of ^{26}Ne based on a recent β decay experiment [18]. The gated decay curves were generated for transitions that were statistically significant, and the half-lives determined in the above-mentioned procedure are given in Table III. The weighted average of the half-life was found to be 192(4) ms, which is in good agreement with previous work [18]. In addition, a weak γ-ray at 2219(4) keV was found which could be the γ-ray transition at 2232(15) keV in ^{26}Na observed

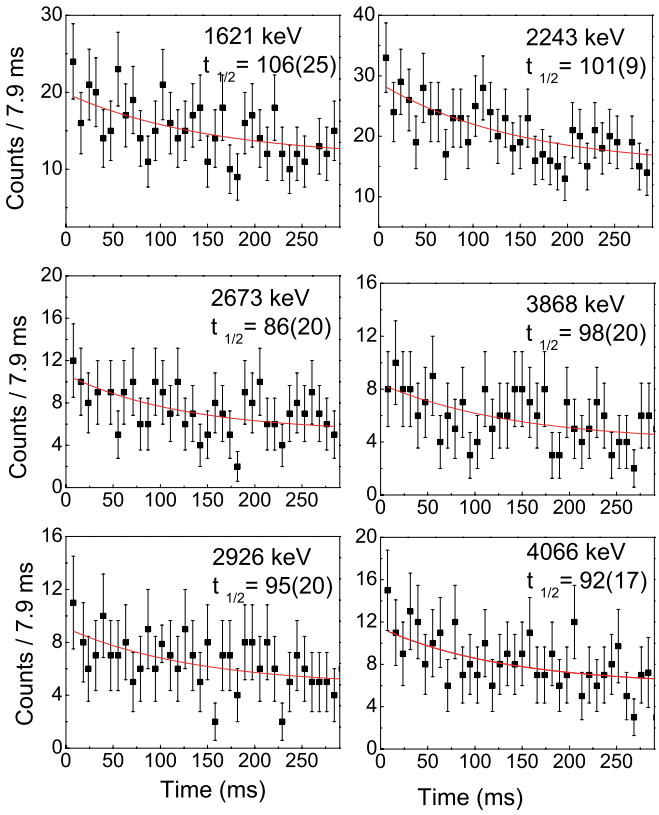

FIG. 4. (Color online) γ-ray gated decay curves, with gated γ-ray peak energies in keV and corresponding gated half-lives in ms. Fitted single exponents are shown for the statistically significant peaks corresponding to β decay of ^{23}O.

TABLE III. γ-ray assignment for β decay of ^{26}Ne.

γ energy (keV)	Gated half-life (ms)	Emission probability (%)	Nuclide	Level (keV)
84(3)	–	95[a]	^{26}Na	84
153(3)	192(4)	3.4(2)	^{26}Na	234
232(2)	193(4)	4.4(2)	^{26}Na	234
404(3)	–	0.4(1)	^{26}Na	404
1212(3)	190(10)	1.2(3)	^{26}Na	2723
1279(3)	–	5.4(2)	^{26}Na	1513
2219(4)	–	0.6(2)	^{26}Na	2219
2486(4)	–	0.7(2)	^{26}Na	2723

[a]From Ref. [18].

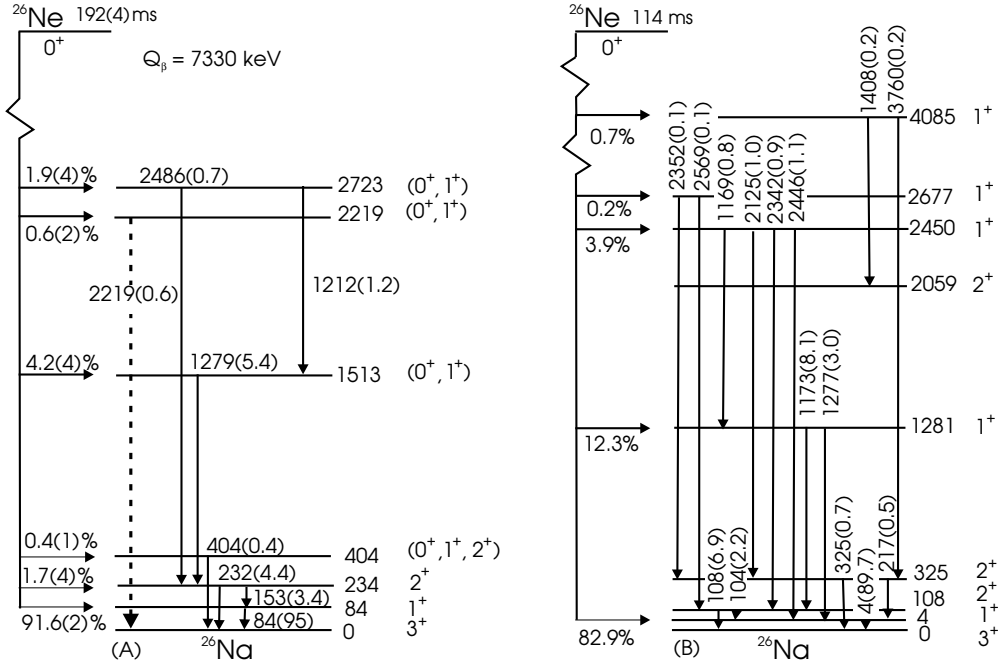

FIG. 5. Decay schemes for ^{26}Ne. (a) Experimental: γ-ray decay (vertical arrows) with the transition energy and emission probabilities in parenthesis. Horizontal arrow shows the β decay feeding to the level with the β branch and the corresponding uncertainty in parenthesis. Dashed arrow shows a new γ-ray transition. Experimental weighted average half-life is given. (b) Theoretical: constructed with a minimum limit of 0.1% for the β branch and γ emission probability. γ-ray decay notation same as in (a); β branch is given on the horizontal arrow. Calculated half-life is 114 ms.

in nuclear reaction studies by Lee *et al*. [19]. The γ-ray at 1996 keV reported in the same work [19] was not seen, although both γ rays were reported to deexcite the same energy level. The emission probability of the 84 keV γ-ray was not determined because of the high threshold of some of the SeGA detectors, thus this value was adopted from Ref. [18] and used in β branch calculations. The level scheme for β decay of ^{26}Ne, shown in Fig. 5(a), has been constructed from the experimental observations. There was no β decay feeding to the ground state of ^{26}Na, as the number of ^{26}Na β decay events deduced from γ-ray activities was in good agreement with the number of γ-ray cascading events to the ^{26}Na ground state.

New shell model calculations for the β decay of ^{26}Ne and ^{26}Na were performed in *sd*-shell model space using new USDB ("universal" sd-type B) interaction [20]. Figure 5(b) shows the ^{26}Ne β decay scheme constructed from the shell model calculations. β decay branches and the γ-ray emission probabilities higher than 0.1% are shown. The comparison of both decay schemes shows reasonable agreement between our data and the shell model calculations. However, Lee *et al*. [19] have argued that older shell model calculations clearly disagree below 3 MeV with the experimental results of the β decay of ^{26}Ne from the work of Weissman *et al*. based on the nonobservation of a 1^+ state in ^{26}Na predicted to have a relatively strong β branch. They also supported their argument by providing a similar situation in the β decay of ^{28}Ne. Our results show that the missing 1^+ state could be the state at 2219 keV. The level ordering obtained by new shell model calculations supports this assignment, although the β feeding does not match as well.

D. β decay scheme of ^{23}O

The assignments of γ-rays to the energy levels in ^{23}F were based on known energy levels and corresponding γ-ray transitions observed in previous experiments, since β-delayed γ-γ coincidence events were not observed because of poor statistics. The γ-ray transition at 638 keV deexcites the energy level at 710 keV in the neutron daughter ^{22}F following Ref. [17]. The γ-ray transitions of 2243, 2926, 3367, 3868, and 4066 keV were assigned to feed the ground state of ^{23}F as reported in Ref. [8]. The γ-rays of 912, 1237, and 2673 keV were placed depopulating the known states at 3837, 4604, and 5599 keV, respectively, to be consistent with the γ-ray decay scheme in ^{23}F as given in Ref. [8]. The 3837 keV state was fed by the γ-ray of 1716 keV originated from the known state at 5553 keV. This tentative placement is reasonable because it matches with the difference in known energy levels and the intensity flow. Although the γ-ray at 1621 keV was not seen in previous experiments, this could be assigned to the 3866 keV state based on the energy difference between the known energy levels at 2243 and 3866 keV. Table IV shows the observed γ-rays with their uncertainties, gated half-lives, γ emission probabilities, and the energy level assignments for the β decay of ^{23}O.

The proposed β decay scheme of ^{23}O, shown in Fig. 6(a), is based on the known energy levels in ^{23}F and the observed energy and intensity sum rules. The absolute β decay branching to each populated level was calculated by taking the difference between γ-ray decay into and out of the level, normalized to the total decay. The branching is shown on horizontal arrows in Fig. 6(a) with uncertainties in parenthesis.

TABLE IV. γ-ray assignment for β decay of ^{23}O.

γ energy (keV)	Gated half-life (ms)	Emission probability (%)	Nuclide	Level (keV)
911(4)	–	2.7(12)	^{23}F	3837
1237(4)	–	3.1(9)	^{23}F	4604
1621(6)	106(25)	5.7(10)	^{23}F	3866
1716(6)	–	2.1(6)	^{23}F	5553
2243(8)	101(9)	51.5(12)	^{23}F	2243
2673(9)	86(20)	5.2(10)	^{23}F	5599
2926(10)	95(20)	7.2(18)	^{23}F	2926
3367(13)	–	4.5(10)	^{23}F	3367
3868(15)	98(20)	10.1(16)	^{23}F	3866
4066(16)	92(17)	17.1(17)	^{23}F	4066
638(3)	–	1.5(8)	^{22}F	710

The γ-ray energies and their emission probabilities in parenthesis are given on the vertical arrows. The γ-ray feeding to the ground state and the total ^{23}F β decay events calculated from the γ-rays associated with ^{23}F decay were consistent within uncertainties. This leaves negligible β decay feeding to the ground state. The β decay branches were not calculated for the states at 2926, 3367, and 3837 keV since the feeding and deexcitation intensities agreed within uncertainties. The observation of the 638 keV γ-ray suggests that β-delayed neutrons could feed the excited state in ^{22}F as shown in Fig. 6(a). The neutron bound states associated with very small β decay feeding and weak γ-ray decay could be existed as the β decay window of 2 MeV is opened in between the highest observed energy state from the present work and the neutron separation energy. The apparent log(ft) values were calculated for the observed states in ^{23}F using the method in Ref. [21] with the measured half-life, the β decay branch (given in Table V), and the Q_β value from Ref. [17]. Table V shows the calculated β decay branches, log(ft) values, and Gamow-Teller transition strengths [B(GT)] for the observed bound states along with their spin and parity assignments. B(GT) values were calculated according to Ref. [22] using the log(ft) values.

Six allowed β decays with the spin and parity assignments of $1/2^+$ or $3/2^+$ are reasonable from the measured log(ft) values and the selection rules of β decay considering the ^{23}O ground state has a $1/2^+$. The states at 2243 and 4066 keV were given spin and parity assignments of $1/2^+$ and $3/2^+$, respectively, to be consistent with the corresponding assignments given by Michimasa *et al.* [8].

Shell model calculations for the β decay of ^{23}O were performed using a USDB interaction and free-nucleon Gamow-Teller operator for β allowed decay. The predictions were done in *sd*-shell model space while considering a $1/2^+$ ground state for ^{23}O. Figure 6(b) shows the β decay scheme for ^{23}O with γ-ray decays and β branches greater than 0.2% deduced from shell model calculations. Our calculations predict nine states that are fed by the allowed β decays

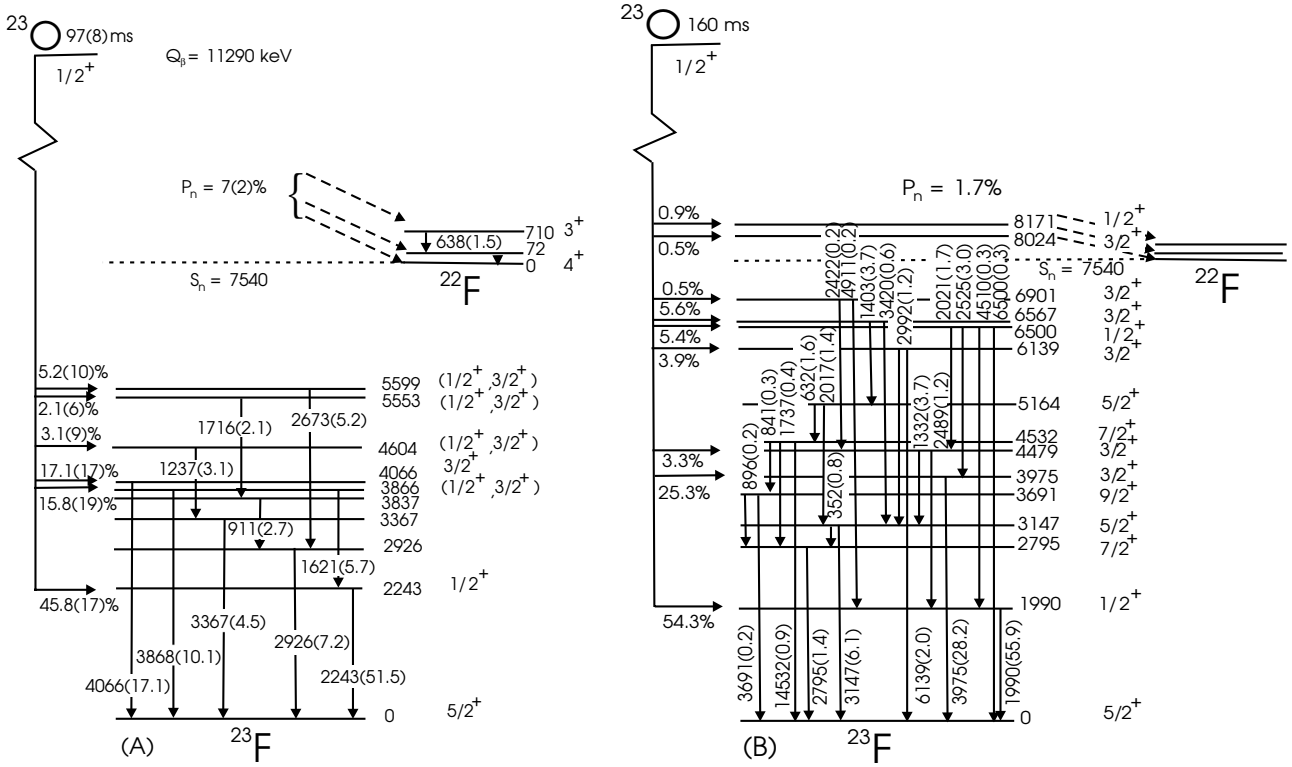

FIG. 6. β decay schemes of ^{23}O. (a) Experimental: γ-ray decay (vertical arrows) with the transition energy and emission probabilities in parenthesis. Horizontal arrow shows the β decay feeding to the level with the β branch and the corresponding uncertainty in parenthesis. The weighted average half-life and P_n value from this experiment, and Q_β value from Ref. [17] are given at the top of scheme. (b) Theoretical: γ-ray emission probabilities and branches higher than 0.2% are shown with the calculated half-life.

TABLE V. Properties of ^{23}O β decay.

Energy level (keV)	Branch (%)	log(ft)	Spin-parity	B(GT)
2243	45.8(17)	4.27	$1/2^+$	0.32
2926	0	–	–	–
3367	0	–	–	–
3837	0	–	–	–
3866	15.8(19)	4.33	$(1/2^+, 3/2^+)$	0.29
4066	17.1(17)	4.24	$3/2^+$	0.36
4604	3.1(9)	4.82	$(1/2^+, 3/2^+)$	0.09
5553	2.1(6)	4.68	$(1/2^+, 3/2^+)$	0.13
5599	5.2(10)	4.28	$(1/2^+, 3/2^+)$	0.32

with branches greater than 0.2%, and two of those states are above the single neutron separation energy leading to neutron decay. The calculations indicate major branches of 54.3% and 25.3% to the states at 1990 ($J^\pi = 1/2^+$) and 3975 keV ($J^\pi = 3/2^+$), respectively. The total neutron emission probability was predicted to be 1.7% with a half-life of 160 ms as shown in Fig. 6(b). In addition, γ-ray decay in ^{23}F, shown in Fig. 6(b), was calculated in the same model space to produce the deexcitation scheme. The overall agreement between the two decay schemes is reasonable within the detection limits.

IV. DISCUSSION

The weighted half-life of 97(8) ms for β decay of ^{23}O measured in this experiment is consistent with the half-life reported by Mueller *et al.* [3], and it is not in good agreement with our predicted value of 160 ms. The half-life obtained with the USDB interaction for the neighboring ^{22}O β decay of 1.4 s is shorter than the experimental value of 2.3(1) s [16]. The ^{22}O half-life shows the typical hindrance of experiment relative to theory for Gamow-Teller decay in the *sd* shell [23]. A similar hindrance is also observed for the ^{26}Ne decay. In contrast, the experimental decay for ^{23}O half-life of 97(8) ms is enhanced relative to theory. The reason for this enhancement is not understood. The total neutron emission probability of 7(2)% from the present work is inconsistent with the experimental values in the literature and also with most of theoretical predictions except for that of Wildenthal *et al.* [5] and our new calculations using USDB interactions of about 2%. The neutron branch was observed by the γ-rays associated with the daughter ^{22}F, and no neutrons were observed with energy above approximately 360 keV.

The level scheme for ^{23}F from the present work can be compared in Fig. 7 with our shell model calculations in *sd*-shell model space and previous experimental work. The first $1/2^+$ state located at 2243 keV is about 253 keV higher than the shell model predicted state at 1990 keV. The level at 4066(16) keV was assigned to be $3/2^+$ in the previous work by Michimasa *et al.* on the basis of spectroscopic factors. Our new shell model calculations also indicate that the state at 3975 keV [24] contains about 50% of the total $d_{3/2}$ spectroscopic strength, thus the calculated 3975 keV state was associated with the observed level at 4066 keV. The next higher shell model state with the spin and parity of $3/2^+$ at 4479 keV should

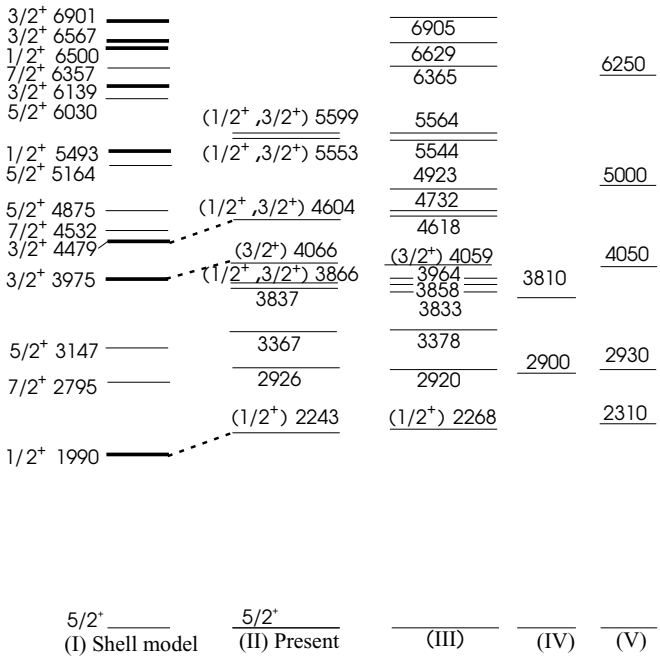

FIG. 7. ^{23}F levels from the present experiment along with present shell model calculations and previous works. Shell model predicted (I) allowed β decay states (thick lines) and forbidden β decay states (thin lines), and the energy levels from the present work (II) and work of Michimasa *et al.* [8] (III), Belleguic *et al.* [1] (IV), and Orr *et al.* [6] (V) are shown. The likely calculated and experimental states are combined with the dotted lines. All energies are given in keV.

be associated with the 4604 keV state. Noting that there are no other low spin states in the calculations near 3.8 MeV and an apparently low spectroscopic factor for the 3858(11) keV state in the work of Michimasa *et al.*, the state observed at 3866(13) keV in this experiment cannot be associated with any of states obtained in the *sd* model space. It could be an intruder state with its observation in β decay due to a strong mixing with the *sd*-shell states. The thick lines in Fig. 7 show the predicted β decay levels in ^{23}F that have β decay branches greater than

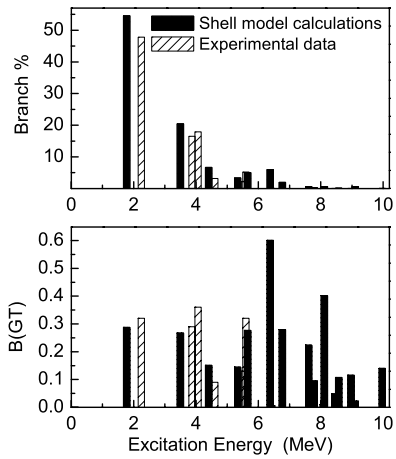

FIG. 8. Comparison of shell model predictions and experimental values of β decay branching (top) and Gamow-Teller strengths (bottom) for the β decay of ^{23}O.

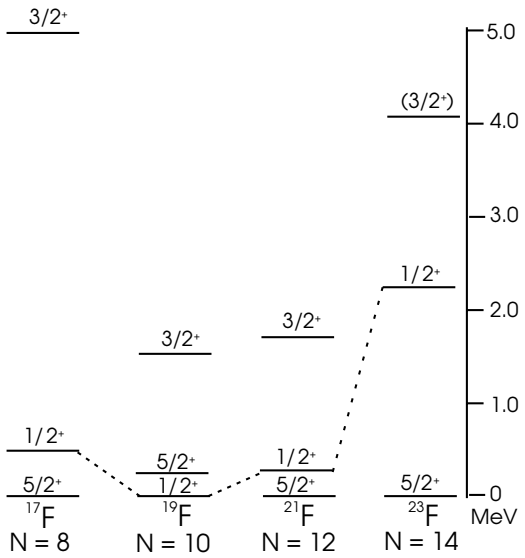

FIG. 9. Location of experimental energy states in odd-mass fluorine isotopes as a function of neutron number.

0.2%. The experimental β decay branching and B(GT) values are compared with the corresponding predicted values in Fig. 8.The experimental values for β decay branching and B(GT) for the first $1/2^+$ state agree reasonably with the shell model predictions. The β decay feeding to the states at 3866 keV and above is not consistent with the calculations. The inconsistency is highlighted by the difference in the B(GT) values.

Figure 9 shows the variation of the energies of the lowest $5/2^+$, $1/2^+$, and $3/2^+$ states in odd-mass fluorine isotopes. The ground states of fluorine isotopes have a single proton in the proton $d_{5/2}$ orbital and fill neutrons into the neutron $d_{5/2}$ orbital as the mass of the isotope increases. The comparison with experimental energy gaps in the fluorine isotopes shows a sudden increase in the gap between $5/2^+$ and $1/2^+$ states in ^{23}F as shown in Fig. 9. This could be an indication of the appearance of $N = 14$ shell closure in this region.

V. SUMMARY

The present work reports the first spectroscopic decay study of ^{23}O, which found a half-life of 97(8) ms and a total neutron emission probability of 7(2)%. Six allowed β decay transitions were observed, including three strong decays to the states at 2243, 3866, and 4066 keV. The comparison of shell model calculations of the β decay showed a reasonable agreement for energies below 4604 keV. The analysis of energy states in fluorine isotopes suggests a widening in the $1/2^+$ and $5/2^+$ energy gap in ^{23}F.

ACKNOWLEDGMENTS

We would like to thank the staff of the NSCL for their assistance during experiments. This work was supported by the National Science Foundation under Grant Nos. PHY-01-10253 and PHY-0555366.

[1] M. Belleguic, M. J. Lòpez-Jiménez, M. Stanoiu, F. Azaiez, M. G. Saint-Laurent, O. Sorlin, N. L. Achouri, J. C. Angélique, C. Bourgeois, C. Borcea *et al.*, Nucl. Phys. **A682**, 136c (2001).
[2] P. G. Thirolf, Phys. Lett. **B485**, 16 (2000).
[3] A. C. Mueller, D. Guillemaud-Mueller, J. C. Jacmart, E. Kashy, F. Pougheon, A. Richard, A. Staudt, H. V. Klapdor-Kleingrothaus, M. Lewitowicz, R. Anne *et al.*, Nucl. Phys. **A513**, 1 (1990).
[4] P. L. Reeder, R. A. Warner, W. K. Hensley, D. J. Vieira, and J. M. Wouters, Phys. Rev. C **44**, 1435 (1991).
[5] B. H. Wildenthal, M. S. Curtin, and B. A. Brown, Phys. Rev. C **28**, 1343 (1983).
[6] N. A. Orr, L. K. Fifield, W. N. Catford, and C. L. Woods, Nucl. Phys. **A491**, 457 (1989).
[7] E. Sauvan, F. Carstoiu, N. A. Orr, J. C. Angélique, W. N. Catford, N. M. Clarke, M. M. Cormick, N. Curtis, M. Freer, S. Grévy, *et al.*, Phys. Lett. **B491**, 1 (2000).
[8] S. Michimasa, S. Shimoura, H. Iwasaki, M. Tamaki, S. Ota, N. Aoi, H. Baba, N. Iwasa, S. Kanno, S. Kubono *et al.*, Phys. Lett. **B638**, 146 (2006).
[9] D. J. Morrissey, B. M. Sherrill, M. Steiner, A. Stolz, and I. Wiedenhoever, Nucl. Instrum. Methods Phys. Res. A **204**, 90 (2003).
[10] http://www.nndc.bnl.gov/ensdf
[11] R. Harkewicz, D. J. Morrissey, B. A. Brown, J. A. Nolen, N. A. Orr, B. M. Sherrill, J. S. Winfield, and J. A. Winger, Phys. Rev. C **44**, 2365 (1991).
[12] C. S. Sumithrarachchi, D. W. Anthony, P. A. Lofy, and D. J. Morrissey, Phys. Rev. C **74**, 024322 (2006).
[13] W. F. Mueller, J. A. Church, T. Glasmacher, D. Gutknecht, G. Hackman, P. G. Hansen, Z. Hu, K. L. Miller, and P. Quirin, Nucl. Instrum. Methods Phys. Res. A **466**, 492 (2001).
[14] P. M. Endt, Nucl. Phys. **A521**, 1 (1990).
[15] H. Bateman, Proc. Cambridge Philos. Soc. **15**, 423 (1910).
[16] L. Weissman, A. F. Lisetskiy, O. Arndt, U. Bergmann, B. A. Brown, J. Cederkall, I. Dillmann, O. Hallmann, L. Fraile, S. Franchoo *et al.*, J. Phys. G **31**, 553 (2005).
[17] R. B. Firestone, Nucl. Data Sheet **106**, 1 (2005).
[18] L. Weissman, O. Arndt, U. Bergmann, J. Cederkall, I. Dillmann, O. Hallmann, L. Fraile, S. Franchoo, L. Gaudefroy, U. Koster *et al.*, Phys. Rev. C **70**, 057306 (2004).
[19] S. Lee, S. L. Tabor, T. Baldwin, D. B. Campbell, I. Calderin, C. Chandler, M. W. Cooper, C. R. Hoffman, K. W. Kemper, J. Pavan *et al.*, Phys. Rev. C **73**, 044321 (2006).
[20] B. A. Brown and W. A. Richter, Phys. Rev. C **74**, 034315 (2006).
[21] N. B. Gove and M. J. Martin, Nucl. Data Tables **A10**, 205 (1971).
[22] K. W. Scheller, J. Gorres, S. Vouzoukas, M. Wiescher, B. Pfeiffer, K. L. Kratz, D. J. Morrissey, B. M. Sherrill, M. Steiner, M. Hellstrom *et al.*, Nucl. Phys. **A582**, 109 (1995).
[23] B. A. Brown and B. H. Wildenthal, At. Data Nucl. Data Table **33**, 347 (1985).
[24] A. Signoracci and B. A. Brown, to be published.